This article was downloaded by:
On: *25 January 2011*
Access details: *Access Details: Free Access*
Publisher *Taylor & Francis*
Informa Ltd Registered in England and Wales Registered Number: 1072954 Registered office: Mortimer House, 37-41 Mortimer Street, London W1T 3JH, UK

Liquid Crystals

Publication details, including instructions for authors and subscription information:
http://www.informaworld.com/smpp/title~content=t713926090

Anomalies of periodicity in TGB structures in new liquid crystal dimers

Soon Wook Cha; Jung-Il Jin; M. F. Achard; F. Hardouin

Online publication date: 11 November 2010

To cite this Article Cha, Soon Wook , Jin, Jung-Il , Achard, M. F. and Hardouin, F.(2002) 'Anomalies of periodicity in TGB structures in new liquid crystal dimers', Liquid Crystals, 29: 6, 755 — 763
To link to this Article: DOI: 10.1080/02678290210129902
URL: http://dx.doi.org/10.1080/02678290210129902

PLEASE SCROLL DOWN FOR ARTICLE

Full terms and conditions of use: http://www.informaworld.com/terms-and-conditions-of-access.pdf

This article may be used for research, teaching and private study purposes. Any substantial or systematic reproduction, re-distribution, re-selling, loan or sub-licensing, systematic supply or distribution in any form to anyone is expressly forbidden.

The publisher does not give any warranty express or implied or make any representation that the contents will be complete or accurate or up to date. The accuracy of any instructions, formulae and drug doses should be independently verified with primary sources. The publisher shall not be liable for any loss, actions, claims, proceedings, demand or costs or damages whatsoever or howsoever caused arising directly or indirectly in connection with or arising out of the use of this material.

LIQUID CRYSTALS, 2002, VOL. 29, NO. 6, 755–763

Anomalies of periodicity in TGB structures in new liquid crystal dimers

SOON WOOK CHA, JUNG-IL JIN
Center for Electro- and Photo-responsive Molecules and Department of Chemistry, Korea University, Seoul 136-701, Korea

M. F. ACHARD* and F. HARDOUIN
Centre de Recherche Paul Pascal, Université Bordeaux I, Av. A. Schweitzer, 33600 Pessac, France

(*Received 6 November 2001; in final form 14 January 2002; accepted 16 January 2002*)

Non-symmetric liquid crystal dimers consist of two different mesogenic units linked through a polymethylene flexible spacer. Our previous studies have shown that dimers containing a cholesteryl moiety as one of the mesogenic groups and a Schiff's base unit as the second, exhibit a rich polymorphism and that several types of smectic packing are obtained depending on the molecular parameters: specifically, a smectic periodicity similar to the molecular length and an intercalated structure with a smectic parameter lower than half the molecular length can be obtained. The competition between these two incommensurate lengths can induce two-dimensional phases and/or an incommensurate smectic phase in which the two smectic periodicities coexist over a long range. Small modifications of the molecular structure can significantly influence the phase sequence. Here we have replaced the Schiff's base by a tolan unit and the terminal alkyl chains by alkoxy chains. As a result, anomalies of periodicity are also observed in this new dimeric series, but they occur mainly in TGB structures.

1. Introduction

The smectic phase behaviour of non-symmetric liquid crystal dimers, consisting of two different mesogenic units linked through a polymethylene spacer, appears rather intriguing. Indeed, within the same series, certain homologues form an intercalated smectic phase, in which the layer spacing is lower than half the molecular length, while other homologues exhibit smectic phases with a periodicity close to or larger than the molecular length [1]. In all these examples, the nature of the smectic phase formed has been found to depend on the relative lengths of the spacer and of the terminal chains [1–3]. Between these two regimes, depending on the series, the smectic phase vanishes [4], or anomalies of periodicity are revealed through the occurrence of two-dimensional modulated phases [3, 5] and, in some rare cases, of an incommensurate fluid smectic phase Sic [5, 6].

For several years, we have focused on dimers composed of a Schiff's base mesogen linked to a cholesteryl moiety by a spacer [2, 6–11]. In these compounds, denoted as KI-*n*(*m*) (where *n* and *m* refer to the number of methylene groups in the spacer and the terminal alkyl chain, respectively), the smectic arrangements appear to be very sensitive to each molecular parameter of the chemical structure. The dependence of the smectic layering on the length of the terminal alkyl chain shows that the short-chained members exhibit intercalated

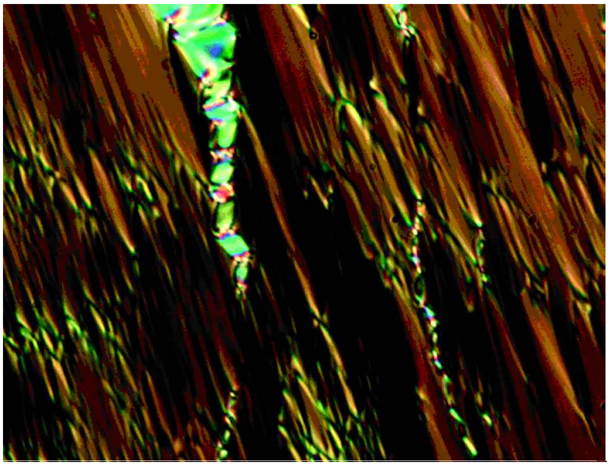

Figure 1. Focal-conic texture of the smectic phase of KI5-T(O3) at 116°C.

---

*Author for correspondence, e-mail: achard@crpp.u-bordeaux.fr

Liquid Crystals ISSN 0267-8292 print/ISSN 1366-5855 online © 2002 Taylor & Francis Ltd
http://www.tandf.co.uk/journals
DOI: 10.1080/02678290210129902

structures (labelled as the 'Sq3' phase), while the longer homologues show a 'dimer' modulation (labelled as 'Sq1' phases) [6]. By contrast, short spacers induce a 'Sq1' packing while long spacers lead to intercalated 'Sq3' smectics [2]. For specific n and m values, this frustration resulting from these two incommensurate lengths induces smectic phases with anomalies of periodicity. For example, KI-5(4) shows intermediate behaviour in which the system crosses over between the two periodicities and forms commensurate 'Sq1' and 'Sq3' phases, incommensurate Sic and two dimensional fluid smectic phases [5, 7]. In the incommensurate smectic phases, the two incommensurate scattering vectors $q1$ and $q3$ are collinear and the two competing periodicities coexist over a long range.

The objective of the present study was to modify the initial KI-n(m) system by replacing the Schiff's base by a tolan unit [9] and the alkyl chains by alkoxy chains ($m = 3$, 4, 5, 6, 10). The pentamethylene spacer is kept constant ($n = 5$). The acronym used to describe these dimers is KI5-T(Om):

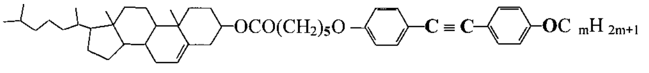

2. Experimental

2.1. *Synthesis*

All of the compounds were synthesized by reacting cholesteryl 6-bromobenzoate with either 4-(4-propoxyphenylethynyl)phenol, 4-(4-butoxyphenylethynyl)phenol, 4-(4-pentyloxyphenylethynyl)phenol, 4-(4-hexyloxyphenylethynyl)phenol, 4-(4-heptyloxyphenylethynyl)phenol or 4-(4-decyloxyphenylethynyl)phenol in N,N-dimethylformamide (DMF) in the presence of a base. Since the synthetic procedure was the same for all the compounds, a representative preparation method is given in detail for KI5-T(O3). Thus, cholesteryl 6-bromobenzoate (1.68 g, 3.0×10^{-3} mol) and 4-(4-propoxyphenylethynyl)phenol (1.0 g, 4.0×10^{-3} mol) were dissolved in DMF (20 ml) containing K_2CO_3 (0.6 g). The mixture was stirred at 120°C for 10 h. The insoluble material was removed by filtration, and the filtrate cooled to room temperature. The precipitate was collected by filtration. The crude product was passed through a short silica gel column using a mixture of ethyl acetate and n-hexane (1 : 5 by volume) as eluent. The yield was 1.6 g (72%).

KI5-T(O3): ^{1}H NMR ($CDCl_3$, δ ppm): 0.65–2.0 (m, 52H, $-CH-$, CH_2- and CH_3-), 2.3 (m, 4H, $-C{=}CH-\underline{CH_2}-$ and $-OCO-\underline{CH_2}-$), 4.0 (m, 4H, $-\underline{CH_2}OAr$), 4.6 (m, 1H, $-O\underline{CH}-$), 5.4 (m, 1H, $-C{=}\underline{CH}-$), 6.9 (d, 2H, 2H, Ar$-\underline{H}$), 7.4 (d, 2H, 2H, Ar$-\underline{H}$). FTIR (KBr, cm^{-1}): 2938 (aliphatic C$-$H stretching), 1730 (C=O stretching), 1253 and 1160 (C$-$O stretching). Anal: calcd for $C_{50}H_{70}O_4$ C 81.70, H 9.60; found C 81.66, H 9.56%.

KI5-T(O4): ^{1}H NMR ($CDCl_3$, δ ppm): 0.65–2.0 (m, 54H, $-CH-$, CH_2- and CH_3-), 2.3 (m, 4H, $-C{=}CH-\underline{CH_2}-$ and $-OCO-\underline{CH_2}-$), 4.0 (m, 4H, $-\underline{CH_2}OAr$), 4.6 (m, 1H, $-O\underline{CH}-$), 5.4 (m, 1H, $-C{=}\underline{CH}-$),

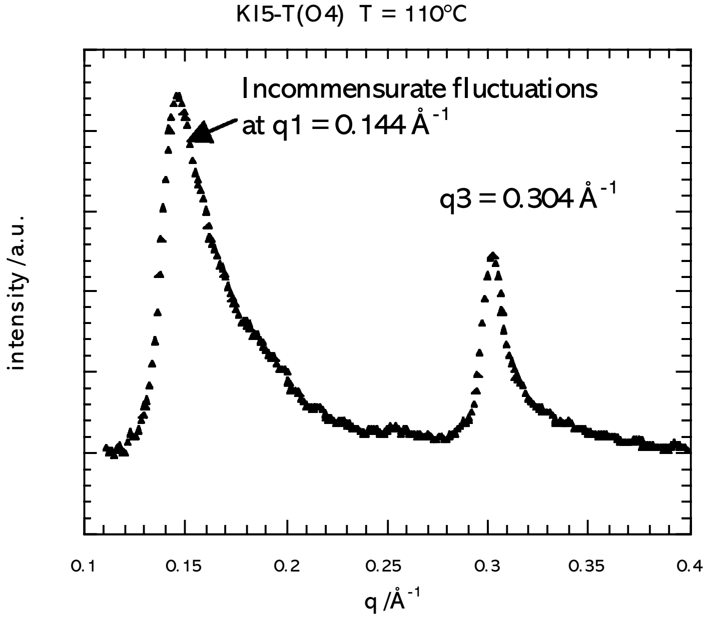

Figure 2. Intensity profile in the low angle region for KI5-T(O4) at 110°C. The Bragg peak observed at $q3 = 0.304$ Å^{-1} corresponds to a smectic parameter of 20.6 Å; the intense diffuse scattering centred around $q1 = 0.144$ Å^{-1} reveals incommensurate fluctuations (i.e. not condensed into a Bragg reflection) corresponding to 43.6 Å.

6.9 (d, 2H, 2H, Ar–$\underline{\mathrm{H}}$), 7.4 (d, 2H, 2H, Ar–$\underline{\mathrm{H}}$). FTIR (KBr, $\mathrm{cm^{-1}}$): 2938 (aliphatic C–H stretching), 1732 (C=O stretching), 1256 and 1160 (C–O stretching). Anal: calcd for $\mathrm{C_{51}H_{72}O_4}$ C 81.77, H 9.69; found C 81.80, H 9.62%.

KI5-T(O5): ^{1}H NMR ($\mathrm{CDCl_3}$, δ ppm): 0.65–2.0 (m, 56H, –CH–, $\mathrm{CH_2}$– and $\mathrm{CH_3}$–), 2.3 (m, 4H, –C=CH–$\underline{\mathrm{CH_2}}$– and –OCO–$\underline{\mathrm{CH_2}}$–), 4.0 (m, 4H, –$\underline{\mathrm{CH_2}}$OAr), 4.6 (m, 1H, –O$\underline{\mathrm{CH}}$–), 5.4 (m, 1H, –C=$\underline{\mathrm{CH}}$–), 6.9 (d, 2H, 2H, Ar–$\underline{\mathrm{H}}$), 7.4 (d, 2H, 2H, Ar–$\underline{\mathrm{H}}$). FTIR (KBr, $\mathrm{cm^{-1}}$): 2940 (aliphatic C–H stretching), 1730 (C=O stretching), 1250 and 1162 (C–O stretching). Anal: calcd for $\mathrm{C_{52}H_{74}O_4}$ C 81.84, H 9.77; found C 81.80, H 9.75%.

KI5-T(O6): ^{1}H NMR ($\mathrm{CDCl_3}$, δ ppm): 0.65–2.0 (m, 58H, –CH–, $\mathrm{CH_2}$– and $\mathrm{CH_3}$–), 2.3 (m, 4H, –C=CH–$\underline{\mathrm{CH_2}}$– and –OCO–$\underline{\mathrm{CH_2}}$–), 4.0 (m, 4H, –$\underline{\mathrm{CH_2}}$OAr), 4.6 (m, 1H, –O$\underline{\mathrm{CH}}$–), 5.4 (m, 1H, –C=$\underline{\mathrm{CH}}$–), 6.9 (d, 2H, 2H, Ar–$\underline{\mathrm{H}}$), 7.4 (d, 2H, 2H, Ar–$\underline{\mathrm{H}}$). FTIR (KBr, $\mathrm{cm^{-1}}$): 2936 (aliphatic C–H stretching), 1733 (C=O stretching), 1255 and 1160 (C–O stretching). Anal: calcd for $\mathrm{C_{53}H_{76}O_4}$ C 81.91, H 9.86; found C 81.88, H 9.82%.

KI5-T(O7): ^{1}H NMR ($\mathrm{CDCl_3}$, δ ppm): 0.65–2.0 (m, 60H, –CH–, $\mathrm{CH_2}$– and $\mathrm{CH_3}$–), 2.3 (m, 4H, –C=CH–$\underline{\mathrm{CH_2}}$– and –OCO–$\underline{\mathrm{CH_2}}$–), 4.0 (m, 4H, –$\underline{\mathrm{CH_2}}$OAr), 4.6 (m, 1H, –O$\underline{\mathrm{CH}}$–), 5.4 (m, 1H, –C=$\underline{\mathrm{CH}}$–), 6.9 (d, 2H, 2H, Ar–$\underline{\mathrm{H}}$), 7.4 (d, 2H, 2H, Ar–$\underline{\mathrm{H}}$). FTIR (KBr, $\mathrm{cm^{-1}}$): 2938 (aliphatic C–H stretching), 1730 (C=O stretching), 1258 and 1156 (C–O stretching). Anal: calcd for $\mathrm{C_{54}H_{78}O_4}$ C 81.97, H 9.94; found C 81.93, H 9.92%.

KI5-T(O10): ^{1}H NMR ($\mathrm{CDCl_3}$, δ ppm): 0.65–2.0 (m, 66H, –CH–, $\mathrm{CH_2}$– and $\mathrm{CH_3}$–), 2.3 (m, 4H, –C=CH–$\underline{\mathrm{CH_2}}$– and –OCO–$\underline{\mathrm{CH_2}}$–), 4.0 (m, 4H, –$\underline{\mathrm{CH_2}}$OAr), 4.6 (m, 1H, –O$\underline{\mathrm{CH}}$–), 5.4 (m, 1H, –C=$\underline{\mathrm{CH}}$–), 6.9 (d, 2H, 2H, Ar–$\underline{\mathrm{H}}$), 7.4 (d, 2H, 2H, Ar–$\underline{\mathrm{H}}$). FTIR (KBr, $\mathrm{cm^{-1}}$): 2942 (aliphatic C–H stretching), 1732 (C=O stretching), 1254 and 1160 (C–O stretching). Anal: calcd for $\mathrm{C_{57}H_{84}O_4}$ C 82.16, H 10.16; found C 82.11, H 10.12%.

2.2. *Characterization*

The IR and ^{1}H NMR spectra of all intermediate and final compounds were recorded on a Bomem MB FTIR spectrophotometer and Bruker AM300 spectrometer, respectively. The thermal behaviour was investigated using a Perkin-Elmer DSC7 differential calorimeter under nitrogen atmosphere. The optical textures of the mesophases were observed through a polarizing microscope (Leitz Diavert) equipped with a hot stage (FP-82HT) and an automatic controller (Mettler FP-90). When the sample formed a homeotropic texture on the regular

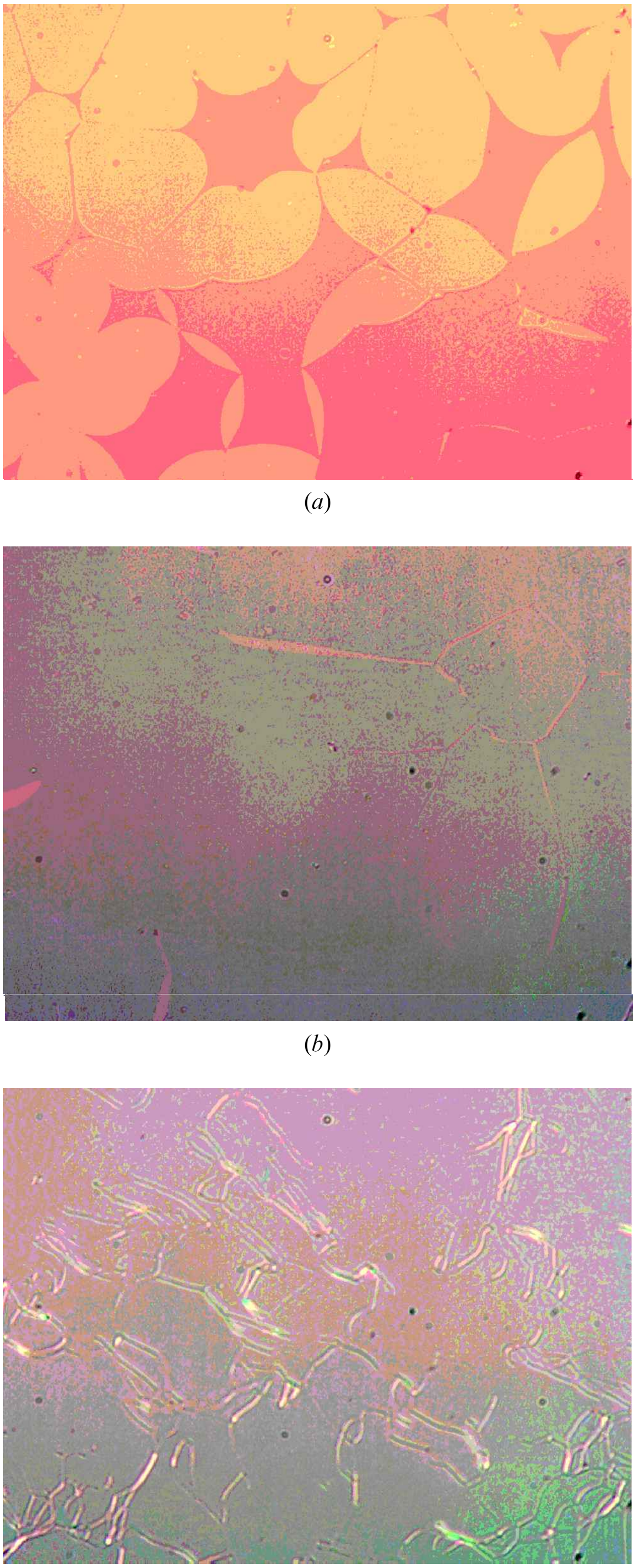
(*a*)

(*b*)

(*c*)

Figure 3. Planar textures of KI5-T(O5) at different temperatures: (*a*) cholesteric phase (*b*) $\mathrm{TGB_A}$ phase at 140°C and (*c*) at 100°C.

slide glass, a rubbed polyimide substrate was used to observe their optical textures. For the X-ray experiments, the CuK$_\alpha$ radiation of a 18 kW rotating anode X-ray generator (Rigaku-200) was selected by a flat (1 1 1) germanium monochromator. The scattered radiation was collected on a two-dimensional detector (Imaging Plate system from Mar Research, Hamburg). The samples were placed in an oven, providing a temperature control of 0.1 K.

3. Results

On cooling from the isotropic liquid, all the homologues exhibit a cholesteric phase, but, and as reported for the Schiff's base KI5-(*m*) series [6], the smectic polymorphism of the tolan dimers KI5-T(O*m*) is strongly dependent on the terminal chain length, *m*. Thus, below the cholesteric mesophase, a twist grain boundary and/or one or two smectic mesophases are observed depending on the value of *m*. It is important to note that although optical microscopy and calorimetric investigations were useful for an initial characterization of the liquid crystalline phases, X-ray diffraction experiments were essential for a complete identification of the mesophases of this series. We now describe the polymorphism determined using these three complementary techniques for short and long chain homologues.

The transition temperatures and associated enthalpy changes of the KI5-T(O*m*) series are summarized in the table.

3.1. *Short chain homologues*

3.1.1. $m = 3$

On cooling the cholesteric phase of the propyloxy compound, a TGB$_A$ phase appeared over a short temperature range (2°C). The assignment of the twist grain boundary phase was made from the observation of the characteristic vermis (no surface treatment) and planar (rubbed polyimide) textures and by the existence of a resolution-limited X-ray peak at low angles. On further cooling, the TGB phase transforms into a smectic A phase; specifically, a homeotropic texture spontaneously develops indicating a uniaxial medium and, as shown in figure 1, focal-conic textures are observed on a rubbed polyimide substrate. These two mesophases (TGB and smectic A) exhibit a Bragg peak in the low angle region and a diffuse scattering centred at $2\pi/5.2\,\text{Å}^{-1}$ in the wide angle domain typical of a liquid-like short range order within the layers. The layer spacing $d = 2\pi/q3 = 20.2$ Å indicates a TGB$_A$ and SmA intercalated structure with a layer parameter d lower than half the molecular length L, estimated considering the molecule in the all-*trans*-conformation ($d/L \approx 0.45$).

In the following, we add to the label of the smectic or TGB phases an index to indicate the type of smectic packing, corresponding to the scattering vector: '$q1$' refers to a layer spacing related to the molecular length of the dimer, while '$q3$' indicates an intercalated smectic with a layer spacing lower than half the dimer length. Using this nomenclature, the KI5-T(O3) homologue displays a N*–TGB$_{Aq3}$–SmA$_{q3}$ sequence.

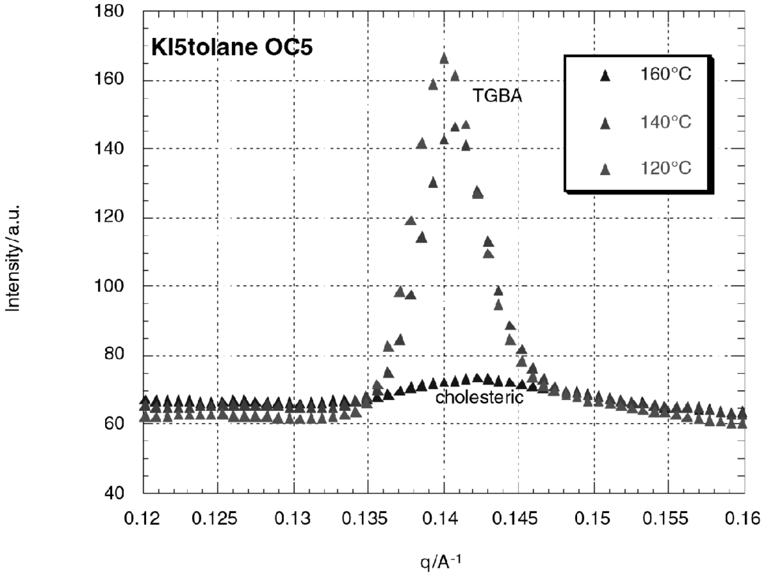

Figure 4. Intensity profile in the low angle region for KI5-T(O5) at 160°C (cholesteric phase) and in the TGB$_{Aq1}$ phase at 140 and 120°C. The Bragg peak observed in the TGB$_A$ phase at $q1 = 0.141\,\text{Å}^{-1}$ corresponds to a smectic parameter of 44.5 Å; this layer parameter slightly increases with decreasing temperature (44.8 Å at 120°C).

Table. Transition temperatures (°C) and enthalpies (J g^{-1}) of the KI-5-T(Om) series. Cr = crystal, SmC* = chiral smectic C phase, SmA = smectic A phase, TGB(A or C) = twist grain boundary phase, N* = cholesteric phase, I = isotropic liquid, [ ] = monotropic mesophase. The enthalpy values are in brackets. When a cholesteric–TGB–smectic sequence is observed, the enthalpy value corresponds to the sum of the N*–TGB and TGB–smectic transition enthalpies. (*) indicates a very low value.

The layered structures (smectic or TGB) are followed by an index indicating the corresponding scattering vector: $q1$ refers to a layer spacing related to the molecular length of the dimer, while $q3$ indicates an intercalated smectic with a layer spacing less than half the dimer length. For details see the text.

m	Transition temperature/°C, and enthalpies/J g^{-1}
3	Cr $\overset{(56)}{126}$ Sm$_{q3}$ 129 $\overset{(*)}{\mathrm{TGB}_{q3}}$ 131 N* $\overset{(6.5)}{206}$ I
4	Cr $\overset{(39)}{113}$ TGB$_{q3}$ $\overset{(*)}{120}$ N* $\overset{(6.9)}{205}$ I
5	Cr $\overset{(49)}{125}$ TGB$_{\mathrm{A}q1}$ $\overset{(*)}{151}$ N* $\overset{(5.8)}{199}$ I
6	Cr $\overset{(47)}{129}$ SmA$_{q1}$ $\overset{(<0.1)}{155}$ TGB$_{\mathrm{A}q1}$ $\overset{(0.4)}{164}$ N* $\overset{(5.9)}{199}$ I
	[TGB$_{\mathrm{C}^*q1}$] $\underset{(*)}{110}$ ↲
7	Cr $\overset{(38)}{114}$ SmA$_{q1}$ 168 TGB$_{\mathrm{A}q1}$ $\overset{(0.9)}{170}$ N* $\overset{(5.5)}{192}$ I
	[SmC$^*_{q1}$] $\underset{(\Delta Cp\,=\,0.02\ \mathrm{J\ g^{-1}})}{113}$ ↲
10	Cr $\overset{(30)}{95}$ SmC$^*_{q1}$ $\overset{(\Delta Cp\,=\,0.03\ \mathrm{J\ g^{-1}})}{132}$ SmA$_{q1}$ $\overset{(1.7)}{183}$ N* $\overset{(6.3)}{186}$ I

3.1.2. $m = 4$

Surprisingly, and as previously observed [12], the butyloxy dimer shows the same planar texture until crystallization, suggesting a wide cholesteric mesophase. However, below 120°C X-ray analysis reveals a low intensity sharp reflection in the low angle region corresponding to a layer spacing $d = 2\pi/q3 = 20.6$ Å suggesting the existence of a TGB$_{q3}$ intercalated phase (figure 2). Note that the N*–TGB$_{q3}$ transition is not detected by DSC but only revealed by X-ray. The X-ray pattern shows a broad diffuse peak at wide angles and hence, it is not a crystalline phase (crystallization is seen at lower temperatures). In addition, and as frequently observed in cholesteryl-based dimers, the 'large' periodicity ($d = 2\pi/q1 = 43.6$ Å) related to the molecular length is also present as strong incommensurate fluctuations in the TGB$_{q3}$ phase of the KI5-T(O4) compound in addition to the $2\pi/q3$ periodicity (figure 2).

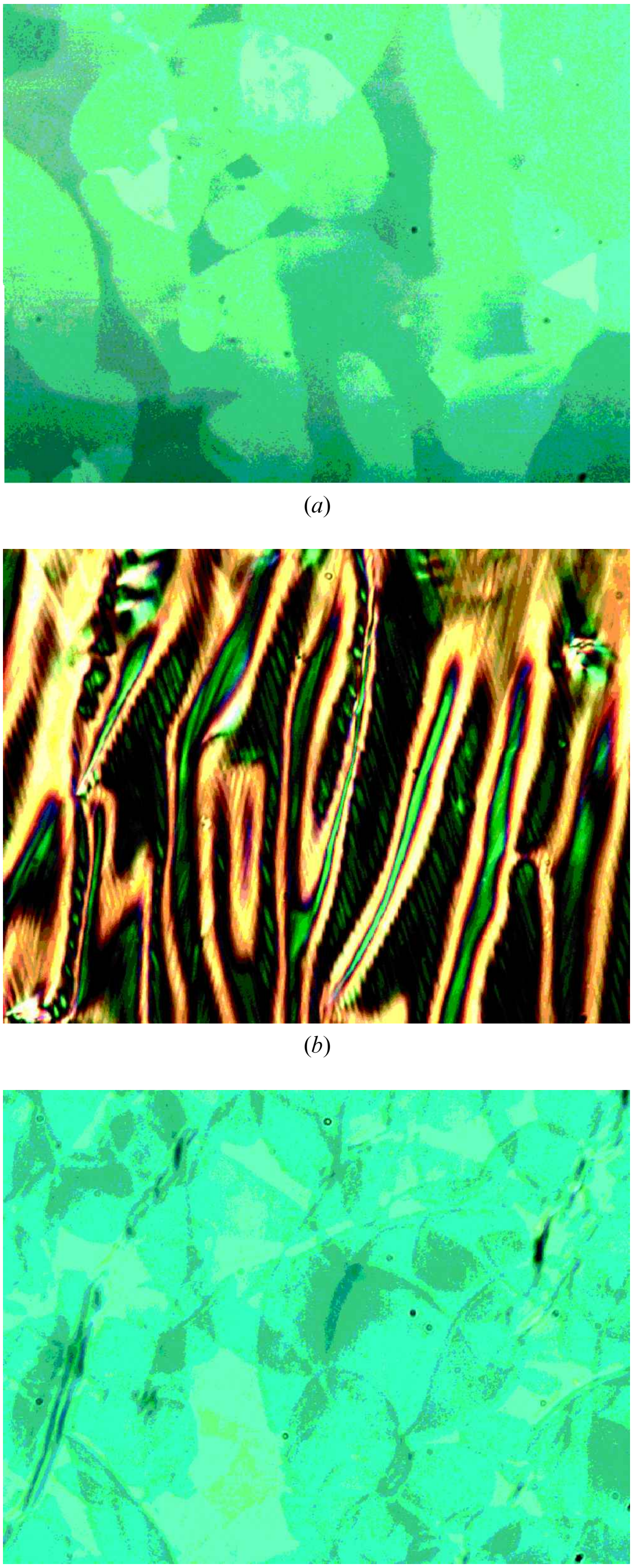

(*a*)

(*b*)

(*c*)

Figure 5. Textures of KI-5T(O6) at (*a*) 147°C, (*b*) 140°C, (*c*) 110°C.

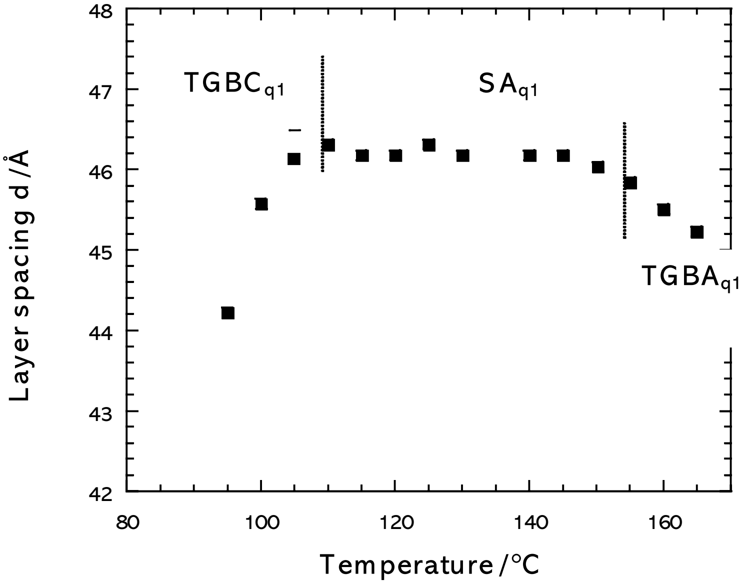

Figure 6. Temperature dependence of the layer spacing for KI5-T(O6).

3.2. *Long chain homologues*

3.2.1. $m=5$

As seen for KI5-T(O4), the pentyloxy homologue shows the planar texture over the whole mesomorphic range (figure 3). This corresponds to a cholesteric phase to 150°C but at lower temperatures to another mesophase detected by X-ray experiments. Indeed, as shown in figure 4, this phase exhibits a sharp reflection in the low angle region, corresponding to a layer spacing $d=2\pi/q1\approx 45$ Å close to the dimer length. The layer spacing slightly increases with decreasing temperature. These observations are consistent with a cholesteric–TGB$_{A_{q1}}$ sequence.

3.2.2. $m=6$

The hexyloxy dimer also displays a cholesteric–TGB$_A$ sequence followed by an additional SmA mesophase at 155°C. Without surface treatment of the glass slides, the TGB phase showed a typical vermis texture and the SmA phase formed homeotropic domains. With rubbed polyimide coated slides, the TGB phase still showed a planar texture, figure 5(*a*), while in the smectic A phase, focal-conics developed, figure 5(*b*). As shown in figure 5(*c*), an unexpected planar texture (or a vermis texture without treatment of the glass slides) was observed at lower temperatures, suggesting either a possible reentrant TGB$_A$ phase or another type of TGB structure.

Over the whole mesomorphic range, X-ray experiments revealed fluid layered structures (i.e. with no order within the layers). At low angles, a sharp reflection corresponds to a layer spacing $d=2\pi/q1$ close to the dimer length. As shown in figure 6, the layer parameter slightly increases with decreasing temperature in agreement with the assignments of TGB$_{A_{q1}}$ and S$_{A_{q1}}$ mesophases, but decreases in the low temperature mesophase. These structural and microscopic observations may correspond to the occurrence of a TGB$_{C^*q1}$ mesophase. Finally, below 96°C a grid texture previously reported for a UTGB$_C^*$ phase [13] is observed until crystallization occurs (figure 7).

3.2.3. $m=7$ *and 10*

More conventional phase sequences are detected for the longer chain homologues ($m=7$ and 10). As for the Schiff's base KI5-(m) series [8], the long terminal chain compounds exhibit two smectic phases. From a textural point of view, the high temperature smectics show focal-conic and homeotropic textures. On cooling into the

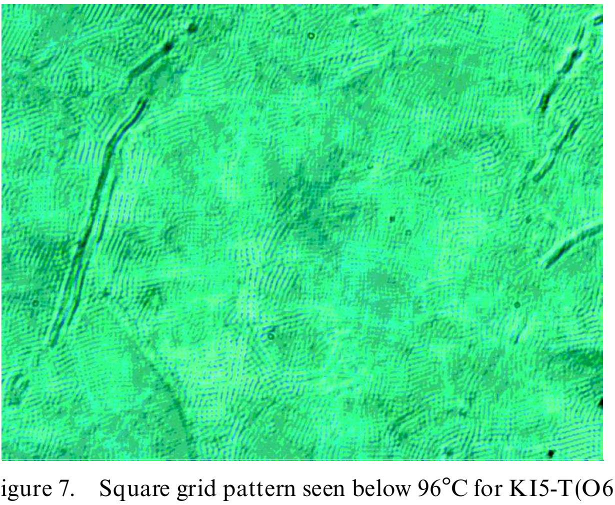

Figure 7. Square grid pattern seen below 96°C for KI5-T(O6) with rubbed polyimide glass plates.

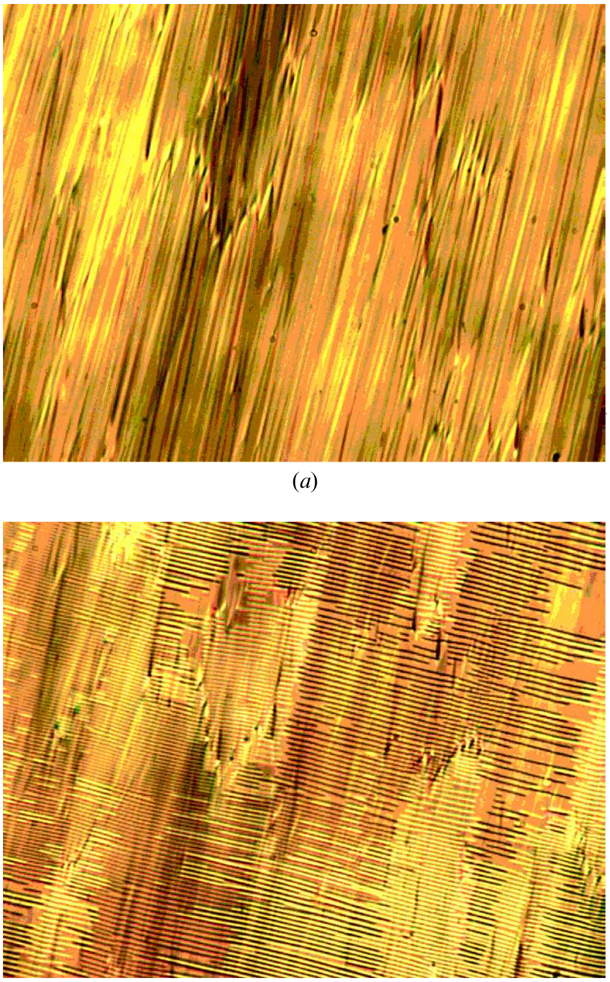
(*a*)

(*b*)

Figure 8. Textures of KI-5T(O7) at (*a*) 115°C, (*b*) 105°C.

low temperature smectic phase, the focal-conic fans become crossed by bars (figure 8) and the homeotropic domains become slightly birefringent. In the DSC scans, this phase change is accompanied by a discontinuity in the heat capacity. X-ray patterns of these smectic phases show a broad diffuse band in the wide angle region indicating disordered smectics. At low angles, both smectic phases are characterized by a sharp reflection with one harmonic. The layer parameter remains constant in the high temperature smectic ($d = 47.2$ Å for $m = 7$ and 51 Å for $m = 10$) and is close to the all-*trans* molecular length estimated from molecular models. As shown in figure 9 the layer spacing significantly decreases with decreasing temperature in the low temperature phase. Thus this analysis shows evidence of a SmA_{q1}–SmC^*_{q1} sequence for the long chain homologues of the KI5-T(O*m*) series in addition to the cholesteric phase. The $m = 7$ compound retains an TGBA_{q1} phase over a short temperature range between the cholesteric and the SmA_{q1} phase.

4. Discussion

Firstly, it can be noted that, as observed in the Schiff's base series, the smectic packing depends on the terminal chain length. An increase of the length of the terminal alkoxy chain causes the smectic periodicity to change from $2\pi/q3$ to $2\pi/q1$. This corresponds to intercalated structures with a layer parameter lower than half the molecular length (d/L ratio ≈ 0.45) for the early members ($m = 3, 4$) while the longer chain compounds ($m = 5$–10) give a packing related to the whole molecule with a d/L ratio close to 1 (figure 10).

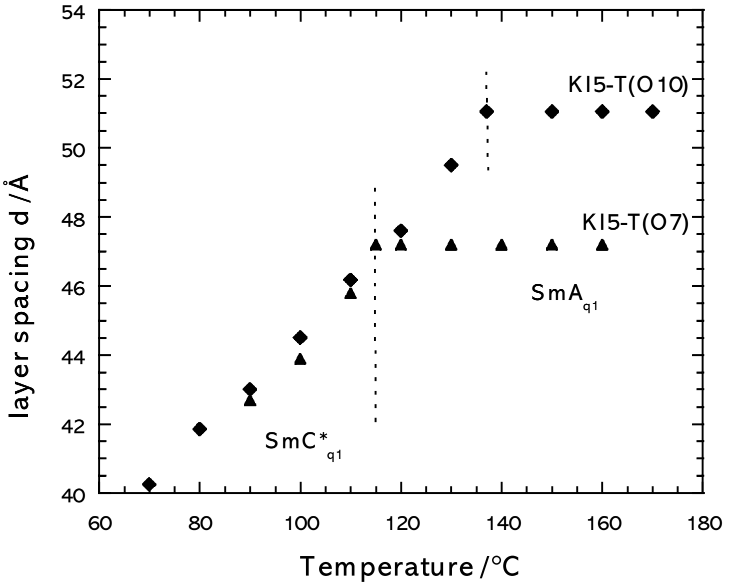

Figure 9. Temperature dependence of the layer spacing *d* (Å) for the long chain homologues of the tolan dimer series.

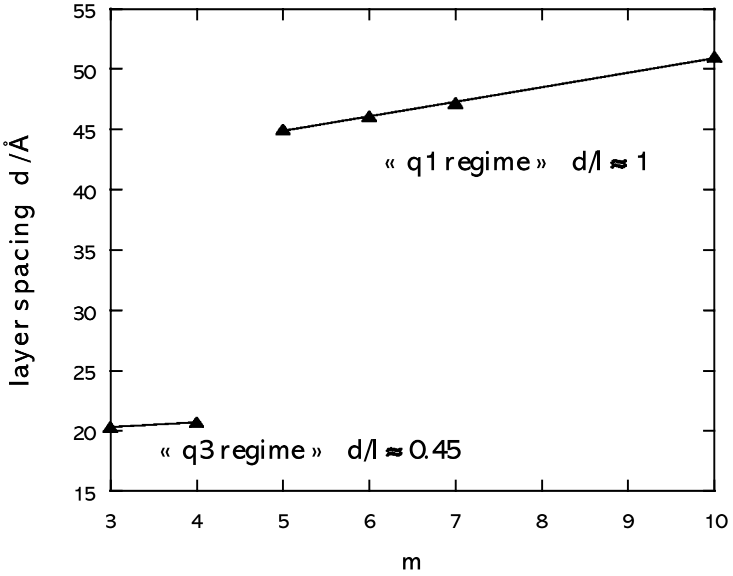

Figure 10. Dependence of the layer spacing on the terminal chain length *m* within the KI5-T(O*m*) series. The *d* value is measured in the higher temperature TGB or smectic phase. There is a linear increase of the layer parameter in the '*q*1' regime on increasing *m* (+ 1.13 Å per additional CH_2 unit).

In the KI5-T(O*m*) series, the change of periodicity occurs between the butyloxy and the pentyloxy homologues, i.e. within a TGB regime of the phase diagram. We can recall that a twist grain boundary phase consists of a helical stack of blocks of smectic liquid crystal, separated by grain boundaries made up of an array of screw dislocations. Since liquid crystals show different kinds of smectics, TGBA (SmA-blocks), TGBC (SmC-blocks with molecules tilted with respect to the layer normal), and TGBC* based on SmC*-like blocks can exist. In addition, however in the case of dimeric compounds, the blocks are based either on intercalated smectics (Sm_{q3}) or on 'monolayer' smectics (Sm_{q1}) giving rise to TGB_{q3} and TGB_{q1} phases, respectively.

We have already shown that an incommensurate smectic phase can be induced in a binary system composed of a dimer which exhibits a Sm_{q3} and another which exhibits a Sm_{q1} mesophase [10]. Therefore, it appears reasonable to assume it is possible to induce an incommensurate smectic packing within a TGB domain, and thus provide evidence for a TGB phase made of blocks of incommensurate smectic. For example, an equimolar mixture of KI5-T(O4) and KI5-T(O5) shows anomalies of periodicity in the TGB domain, as revealed by the simultaneous existence of two incommensurate wave vectors $q1 = 0.141\ \text{Å}^{-1}$ and $q3 = 0.300\ \text{Å}^{-1}$ (figure 11). As previously observed in the Schiff's base series, the corresponding periodicities $2\pi/q1$ and $2\pi/q3$ are related

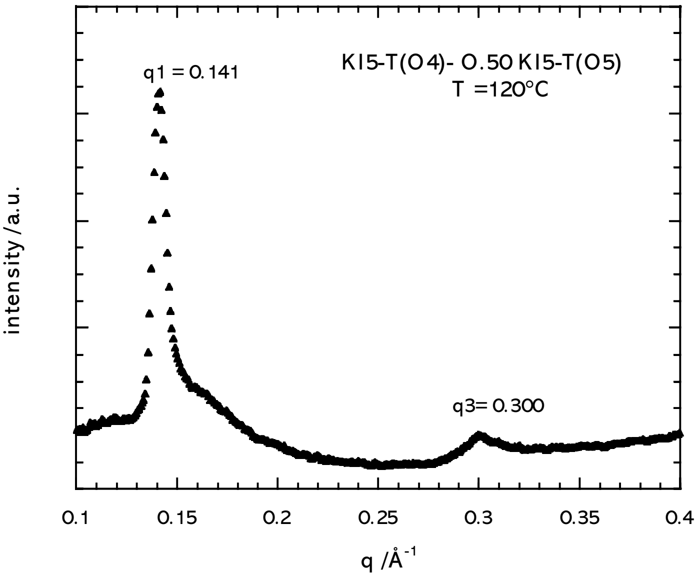

Figure 11. Intensity profile of the X-ray pattern in the low angle region for an equimolar mixture of KI5-T(O4) and KI5-T(O5) in a TGB phase ($T = 120°C$).

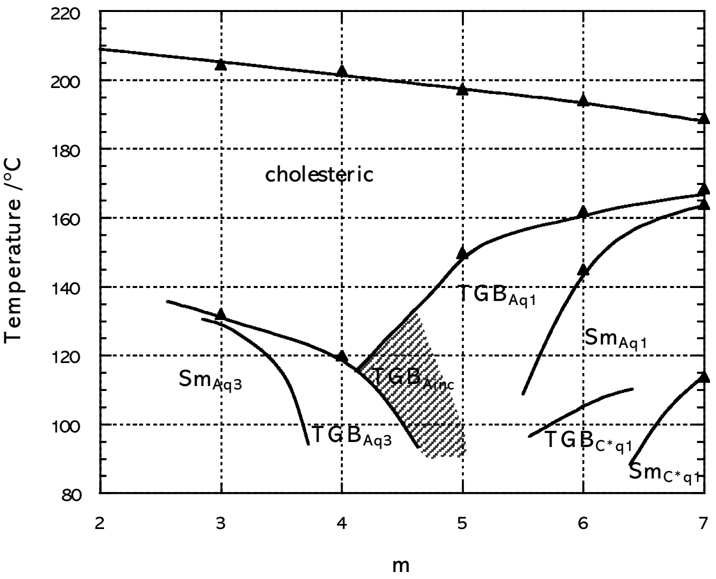

Figure 12. Anomalies of periodicity and occurrence of the TGB structures within the KI5-T(O*m*) series.

to the whole molecule and to the cholesteryl segment, respectively. This preliminary result suggests, as shown in figure 12, the existence of an incommensurate TGB$_{Ainc}$ domain in this tolan dimer series. Additional high resolution X-ray experiments on oriented films of these dimers are currently in progress.

This France–Korea joint research was supported by CNCR and KOSEF. S.W.C. was a recipient of a BK21 fellowship.

References

[1] Attard, G. S., Date, R. W., Imrie, C. T., Luckhurst, G. R., Roskilly, S., Seddon, J. M., and Taylor, L., 1994, *Liq. Cryst.*, **16,** 529.
[2] Hardouin, F., Achard, M. F., Jin, J.-I., and Yun, Y.-K., 1995, *J. Phys II (Fr.)*, **5,** 927.
[3] Faye, V., Nguyen, H. T., and Barois, P., 1997, *J. Phys. II (Fr.)*, **7,** 1245.
[4] Hogan, J. L., Imrie, C. T., and Luckhurst, G. R., 1988, *Liq. Cryst.*, **3,** 645.
[5] Hardouin, F., Achard, M. F., Jin, J.-I., Yun, Y.-K., and Chung, S. J., 1998, *Eur. Phys. J. B*, **1,** 47.
[6] Jin, J.-I., 1995, *Mol. Cryst. liq. Cryst.*, **267,** 249.
[7] Hardouin, F., Achard, M. F., Jin, J.-I., Shin, J.-W., and Yun, Y.-K., 1994, *J. Phys. II (Fr.)*, **4,** 627.
[8] Hardouin, F., Achard, M. F., Laguerre, M., Jin, J.-I., and Ko, D.-H., 1999, *Liq. Cryst.*, **26,** 589.
[9] Cha, S. W., Jin, J.-I., Laguerre, M., Achard, M. F., and Hardouin, F., 1999, *Liq. Cryst.*, **26,** 1325.
[10] Lee, D. W., Jin, J.-I., Laguerre, M., Achard, M. F., and Hardouin, F., 2000, *Liq. Cryst.*, **27,** 145.
[11] Lee, J. W., Jin, J.-I., Achard, M. F., and Hardouin, F., 2001, *Liq. Cryst.*, **28,** 663.
[12] Yelamaggad, C. V., 1999, *Mol. Cryst. liq. Cryst.*, **326,** 149.
[13] Pramod, P. A., Pratibha, R., and Madhusudana, N. V., 1997, *Curr. Sci.*, **73,** 761.